

Time-reversal symmetry breaking superconductivity in three-dimensional Dirac semimetallic silicides

Sudeep K. Ghosh ^{1,*†} P. K. Biswas,^{2,*} Chunqiang Xu,^{3,4} B. Li ⁵ J. Z. Zhao,⁶ A. D. Hillier ^{2,‡} and Xiaofeng Xu ^{3,§}

¹*School of Physical Sciences, University of Kent, Canterbury CT2 7NH, United Kingdom*

²*ISIS Pulsed Neutron and Muon Source, STFC Rutherford Appleton Laboratory, Harwell Campus, Didcot, Oxfordshire OX11 0QX, United Kingdom*

³*Key Laboratory of Quantum Precision Measurement of Zhejiang Province,*

Department of Applied Physics, Zhejiang University of Technology, Hangzhou 310023, China

⁴*School of Physics and Key Laboratory of MEMS of the Ministry of Education, Southeast University, Nanjing 211189, China*

⁵*Information Physics Research Center, Nanjing University of Posts and Telecommunications, Nanjing 210023, China*

⁶*Co-Innovation Center for New Energetic Materials, Southwest University of Science and Technology, Mianyang 621010, China*



(Received 8 December 2021; revised 11 February 2022; accepted 27 February 2022; published 15 March 2022)

Superconductors with broken time-reversal symmetry represent arguably one of the most promising venues for realizing highly sought-after topological superconductivity that is vital to fault-tolerant quantum computation. Here, by using extensive muon-spin relaxation and rotation measurements, we report that the isostructural silicide superconductors (Ta, Nb)OsSi spontaneously break time-reversal symmetry at the superconducting transition while surprisingly showing a fully gapped superconductivity characteristic of conventional superconductors. The first-principles calculations show that (Ta, Nb)OsSi are three-dimensional Dirac semimetals protected by nonsymmorphic symmetries. Taking advantage of the exceptional low symmetry crystal structure of these materials, we have performed detailed theoretical calculations to establish that the superconducting ground state for both (Ta, Nb)OsSi is most likely a nonunitary triplet state.

DOI: [10.1103/PhysRevResearch.4.L012031](https://doi.org/10.1103/PhysRevResearch.4.L012031)

I. INTRODUCTION

Dirac or Weyl semimetals have attracted significant research interest due to their exceptional physical properties arising from the topologically protected gapless electronic excitations [1,2]. Three-dimensional (3D) Dirac semimetals are particularly interesting because they can induce novel topological phases when symmetries are broken, e.g., a Dirac semimetal transforms into a Weyl semimetal with time-reversal symmetry (TRS) breaking [1]. However, research on topological semimetals to date has been primarily focused on characterizing the underlying nontrivial band topology, while their interplay with correlated electronic states, such as novel magnetism and unconventional superconductivity, remained largely an uncharted territory. On the other hand, an interesting class of unconventional superconductors includes the ones that spontaneously break TRS in the superconducting state [3] yet otherwise have properties similar to conventional BCS-type superconductors. As a result, superconducting 3D

Dirac semimetals that break TRS in the superconducting state represent a unique class of materials to realize novel topological superconductivity [4] but are extremely rare.

A superconducting order parameter which breaks TRS is, generically, required to have multiple components with nontrivial phases in between [3]. Such a multicomponent order parameter arises from a multidimensional irreducible representation [5,6] of the crystal point group of the material. However, it is usually difficult to unambiguously establish the structure of the superconducting order parameters for the TRS-breaking superconductors mainly due to two reasons: (a) lack of sufficient knowledge of the electron pairing mechanism and (b) highly symmetric crystal structures leading to many possibilities with similar low-temperature properties. This limits our ability to work by the process of elimination. For example, the point group D_{4h} of Sr_2RuO_4 allows for 20 possibilities with weak spin-orbit coupling (SOC) and 2 possibilities with strong SOC, of TRS-breaking superconducting instabilities [5,6]. In this regard, the superconductors LaNiC_2 [7,8], LaNiGa_2 [9–12], and UTe_2 [13] are exceptions due to their very low-symmetry crystal structure that leads only to a few symmetry-allowed superconducting order parameters. In contrast to LaNiC_2 [8] and LaNiGa_2 [10,11], which show two full gaps, UTe_2 shows nodal behavior [14] in their respective TRS-breaking superconducting state.

The recently discovered osmium-based silicide superconductors (Ta, Nb)OsSi [15] have a very low-symmetry crystal structure as well and weak electron-phonon coupling [16]. In this Letter, by a combination of multiple

*These authors contributed equally to this work.

†S.Ghosh@kent.ac.uk

‡adrian.hillier@stfc.ac.uk

§xuxiaofeng@zjut.edu.cn

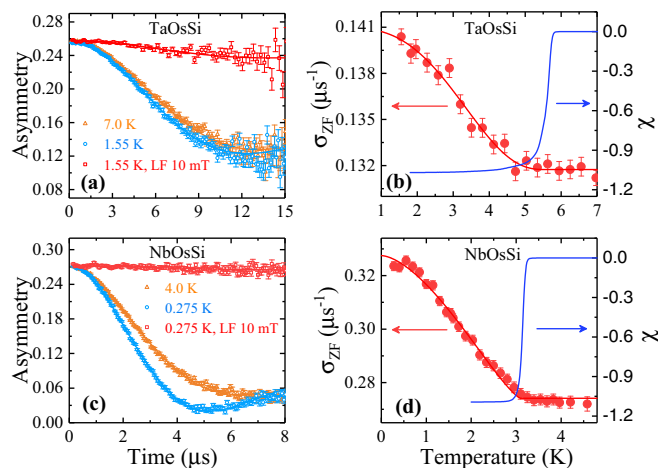


FIG. 1. Time-reversal symmetry breaking observed in (Ta, Nb)OsSi by ZF- μ SR measurements. (a) and (c) ZF- μ SR time spectra collected above and below T_c for TaOsSi and NbOsSi, respectively. The solid lines are the fits to the data using Eq. (1). (b) and (d) The temperature dependence of the muon spin relaxation rate σ_{ZF} of TaOsSi and NbOsSi, respectively. Both show a clear systematic increase in σ_{ZF} just below T_c . The corresponding T_c s are shown in the diamagnetic shifts in the magnetic susceptibility data of the two materials by the solid blue lines. The error bars shown are the standard deviations in the respective measurements.

experimental techniques including muon-spin rotation and relaxation (μ SR) and thermodynamic measurements along with a detailed theoretical analysis, we demonstrate that (Ta, Nb)OsSi are nonsymmorphic symmetry-protected 3D Dirac semimetals that spontaneously break TRS at the superconducting transition but behave as conventional superconductors otherwise. By means of symmetry analysis and model calculations, our observations are found to be consistent with a nonunitary triplet superconducting ground state, the verification of which shall stimulate further study, both experimentally and theoretically.

II. RESULTS AND DISCUSSION

(Ta, Nb)OsSi crystallize in a TiNiSi-type centrosymmetric orthorhombic crystal structure and have similar physical and chemical properties [15]. We prepared polycrystalline samples of (Ta, Nb)OsSi using conventional solid state reaction method and systematically investigated their physical properties using detailed μ SR measurements in zero-field (ZF), longitudinal-field (LF), and transverse-field (TF) modes; magnetic-susceptibility, specific-heat, and electrical-resistivity measurements [17]. The μ SR measurements were performed using the MUSR spectrometer at the ISIS Pulsed Neutron and Muon Source, UK. The temperature dependence of the magnetic susceptibility, collected in zero-field-cooled mode on the same samples, is shown by the solid blue lines on the right axis of Fig. 1(b) [Fig. 1(d)] for TaOsSi (NbOsSi). It indicates bulk superconductivity with $T_c \approx 5.5$ K in TaOsSi and $T_c \approx 3.1$ K in NbOsSi.

ZF- μ SR: ZF- μ SR measurements were performed in search for spontaneous magnetic fields that can appear in the superconducting state leading to breaking of TRS.

Figures 1(a) and 1(c) show the ZF- μ SR time spectra for TaOsSi and NbOsSi, respectively, collected above and below the respective T_c s. A clear increase in the muon-spin relaxation rate in the superconducting state compared to the normal state is evident from both figures. The ZF- μ SR time spectra over a range of temperatures across the T_c for both materials were collected. The data were fitted using a Gaussian Kubo-Toyabe relaxation function [18] $\mathcal{G}(t) = \frac{1}{3} + \frac{2}{3}(1 - \sigma_{ZF}^2 t^2) \exp(-\sigma_{ZF}^2 t^2 / 2)$ multiplied by an exponential decay giving rise to the asymmetry function

$$A(t) = A(0)\mathcal{G}(t)\exp(-\lambda_{ZF}t) + A_{bg}. \quad (1)$$

$A(0)$ and A_{bg} are the initial and background asymmetries of the ZF- μ SR time spectra. σ_{ZF} and λ_{ZF} represent the muon spin relaxation rates originating from the presence of nuclear and electronic moments in the sample, respectively. In the fitting process, the electronic relaxation rate λ_{ZF} was found to be nearly temperature independent for both materials with small average values of $0.0243(2) \mu\text{s}^{-1}$ for TaOsSi and $0.0633(5) \mu\text{s}^{-1}$ for NbOsSi and hence was kept fixed. This indicates the absence of fast-fluctuating electronic moments. The nuclear relaxation rate $\sigma_{ZF}(T)$ shown in Fig. 1(b) [Fig. 1(d)] for TaOsSi (NbOsSi), on the other hand, shows a clear systematic increase just below T_c . The LF- μ SR measurements performed under a field-cooled condition with a small field of 10 mT shown in Figs. 1(a) and 1(c) clearly rule out the possibility of defect- or impurity-induced relaxations since the small field is enough to decouple the muon spins from the weak relaxation channels in both samples. This demonstrates that the increase in σ_{ZF} just below T_c is due to very weak fields which are static or quasistatic on the timescale of muon lifetime and are closely tied to the superconducting state, providing conclusive evidence of spontaneously broken TRS in the superconducting ground states of (Ta, Nb)OsSi. The spontaneous field estimated from the change $\Delta\sigma_{ZF} = \sigma_{ZF}(T \approx 0) - \sigma_{ZF}(T > T_c)$ is $B_{\text{int}} \approx \sqrt{2}\Delta\sigma_{ZF}/\gamma_\mu = 0.17$ G (0.83 G) for TaOsSi (NbOsSi) which is similar to other TRS-breaking superconductors [3]. Here, $\gamma_\mu = 2\pi \times 135.5$ MHz/T is the muon gyromagnetic ratio [19].

TF- μ SR: To determine the superconducting gap symmetry of (Ta, Nb)OsSi, we have performed extensive TF- μ SR measurements in a transverse field of 30 mT applied above T_c and cooled to the base temperature to stabilize a well-ordered flux-line lattice in the mixed state of the superconductors. The TF- μ SR asymmetry signals collected above and below T_c are shown in Fig. 2(a) [Fig. 2(d)] for TaOsSi (NbOsSi). For both materials, the asymmetry signals above T_c show very little relaxation due to the transverse component of weak nuclear moments present in these materials, while those below T_c show higher relaxation due to the added inhomogeneous field distribution of the flux-line lattice. The TF- μ SR asymmetry signals were analyzed using a Gaussian damped sinusoidal function plus a nondecaying oscillation that contributes to the muons stopping in the silver sample holder:

$$A_{\text{TF}}(t) = A(0)\exp(-\sigma^2 t^2 / 2)\cos(\gamma_\mu \langle B \rangle t + \phi) + A_{\text{bg}}\cos(\gamma_\mu B_{\text{bg}} t + \phi). \quad (2)$$

Here $A(0)$ and A_{bg} are the initial sample and background asymmetries, respectively, $\langle B \rangle$ and B_{bg} are the average in-

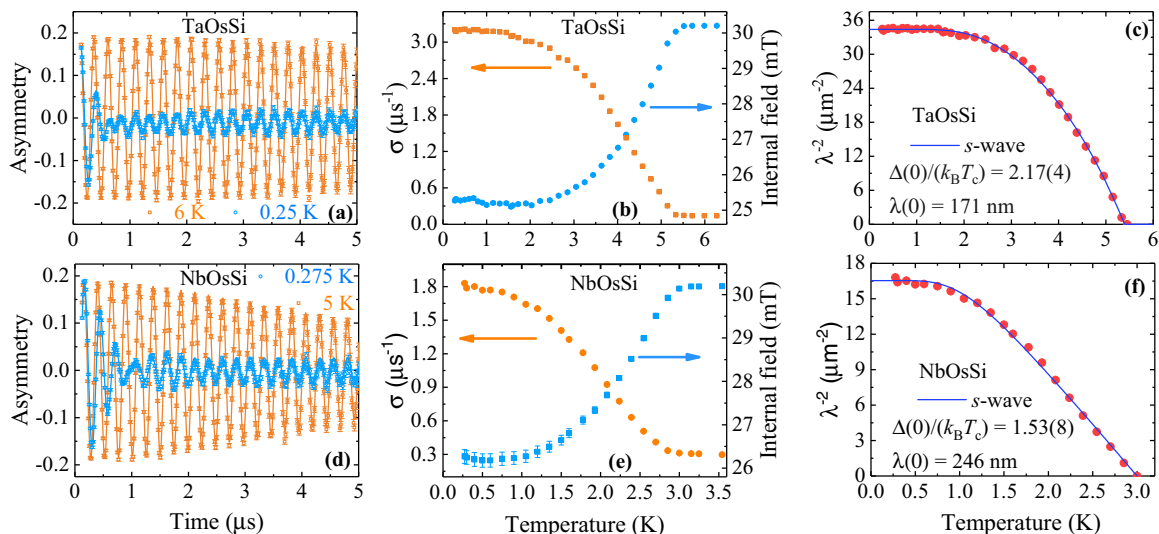


FIG. 2. Characterizing the superconducting properties of (Ta, Nb)OsSi by TF- μ SR measurements. (a) and (d) TF- μ SR time spectra, collected above (red square) and below (blue circle) the T_c in a field-cooled transverse field of 30 mT for TaOsSi and NbOsSi, respectively. The solid lines are the fits to the data using Eq. (2). (b) and (e) The temperature dependence of the extracted relaxation rate σ (left axis) and internal field (right axis) for TaOsSi and NbOsSi, respectively. (c) and (f) The temperature dependence of the inverse magnetic penetration depth squared or equivalently the superfluid density $\rho_s \propto \lambda^{-2}(T)$ for TaOsSi and NbOsSi, respectively. The solid lines are fits to the data with an isotropic single-gap s -wave model.

ternal and background magnetic fields, respectively, ϕ is the shared phase offset, and σ is the depolarization rate of the muon spin precession signal originating from the variance of the magnetic-field distribution in the superconductor. Figures 2(b) and 2(e) show the temperature dependence of the relaxation rate σ (left axis) and internal field (right axis) of TaOsSi and NbOsSi, respectively, extracted from the fits to the asymmetry signals using Eq. (2). The internal fields at the muon sites show strong diamagnetic shifts below T_c for both materials, a clear indication of bulk superconductivity. The $\sigma = (\sigma_{sc}^2 + \sigma_{nm}^2)^{1/2}$ includes contributions from both the flux-line lattice σ_{sc} and a temperature-independent relaxation due to nuclear moments $\sigma_{nm} = 0.146 \mu s^{-1}$ ($0.312 \mu s^{-1}$) for TaOsSi (NbOsSi), determined from the average values of σ collected above the respective T_c s where it is mostly temperature independent.

The London magnetic penetration depth λ can be computed from σ_{sc} within a Ginzburg-Landau treatment of the vortex state in a superconductor in the limit of the applied field $H \ll H_{c2}$ [20] as

$$\frac{\sigma_{sc}(T)}{\gamma_\mu} = 0.06091 \frac{\Phi_0}{\lambda^2(T)}, \quad (3)$$

where $\Phi_0 = 2.068 \times 10^{-15}$ Wb is the flux quantum. The temperature dependence of λ^{-2} extracted using the above equation for TaOsSi and NbOsSi are presented in Figs. 2(c) and 2(f), respectively. Since $\lambda^{-2}(T)$ is a measure of the superfluid density $\rho_s \propto \lambda^{-2} \propto n_s/m^*$ (n_s is the charge carrier concentration, and m^* is the effective mass of the charge carriers), it bears signatures of the symmetry of the superconducting gap. We note from Figs. 2(c) and 2(f) that the superfluid density of both materials shows saturation below $T_c/3$ which indicates the absence of low-lying excited states close to zero temperature, a hallmark of nodeless superconductivity.

To understand the superconducting pairing symmetry, we analyze the temperature dependence of the superfluid density within the local London approximation [$\lambda(0) \gg \xi$, ξ is the coherence length] [21] by

$$\frac{\lambda^{-2}(T)}{\lambda^{-2}(0)} = 1 + 2 \left\langle \int_{\Delta_k(T)}^{\infty} \left(\frac{\partial f}{\partial E} \right) \frac{E dE}{\sqrt{E^2 - |\Delta_k(T)|^2}} \right\rangle_{FS}. \quad (4)$$

Here $\Delta_k(T)$ is the form of the gap function for a given pairing model, $f(E, T) = [1 + \exp(E/k_B T)]^{-1}$ is the Fermi function, and $\langle \rangle_{FS}$ represents an average over a spherical Fermi surface. For an isotropic single gap s -wave model, $\Delta_k(T)$ is independent of k and its temperature dependence is given by [22]

$$\Delta(T) = \Delta(0) \tanh [1.82 \{1.018(T_c/T - 1)\}^{0.51}]. \quad (5)$$

The solid lines in Figs. 2(c) and 2(f) show that the superfluid density can be fitted quite well with an isotropic single-gap s -wave model both for TaOsSi and NbOsSi, respectively. We note that the values of the fitting parameter $\frac{\Delta(0)}{k_B T_c}$ for both (Ta, Nb)OsSi are close to its weak-coupling BCS limit value.

Band structure and specific heat: The space group of (Ta, Nb)OsSi is $Pnma$ (No. 62) and the point group is D_{2h} . The first Brillouin zone with the high-symmetry directions marked is shown in Fig. 3(a). $Pnma$ is a nonsymmorphic space group having three glide planes: $G_1 = \{m_{(0,1,0)}|t_{(0,1/2,0)}\}$, $G_2 = \{m_{(0,0,1)}|t_{(1/2,0,1/2)}\}$, and $G_3 = \{m_{(1,0,0)}|t_{(1/2,1/2,1/2)}\}$, where m and t denote the mirror plane and fractional translation parallel to the plane, respectively. Twofold degeneracies along the high symmetry lines XS , XU , UR , and RS result from G_2 and that along YS and UZ result from G_3 [17]. The band structure of NbOsSi (which is similar to that of TaOsSi [16,23]) computed using density functional theory within the generalized gradient approximation is shown in Fig. 3(c) with and without the effect of SOC. We note that SOC leads to small yet finite splitting of the bands near the Fermi level with

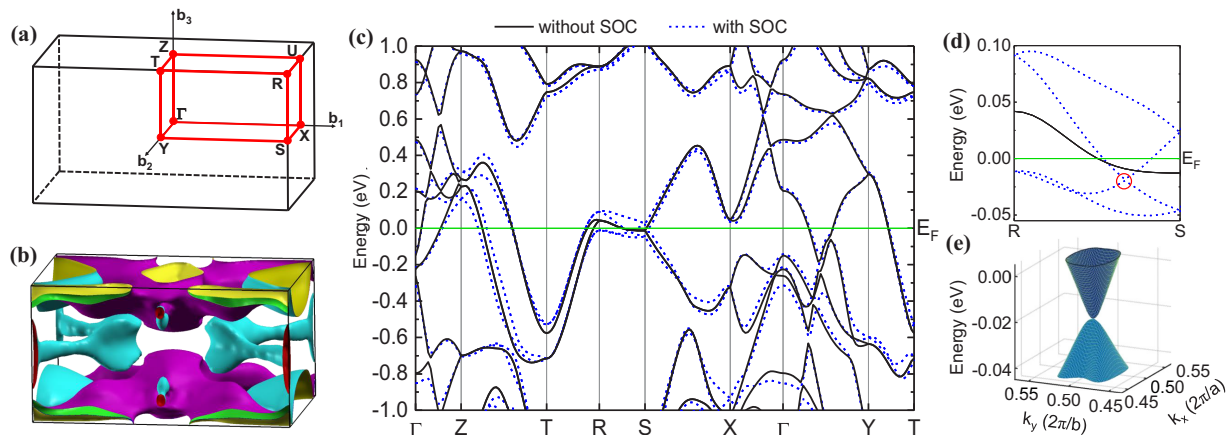


FIG. 3. Band structure of NbOsSi. (a) First Brillouin zone with the high symmetry points marked. (b) Combined view of all the four Fermi surface sheets of NbOsSi without SOC. The large parallel sections of the Fermi surface sheets are clearly visible. (c) The band structure of NbOsSi with and without considering SOC. (d) Enlarged view of the band structure along the RS direction. The Dirac point is marked by the red circle. (e) The dispersion close to the Dirac point marked in (d).

a maximum splitting ~ 100 meV near the R point (maximum splitting ~ 140 meV near the S point for TaOsSi [23]).

(Ta, Nb)OsSi are inherently multiband systems with the Nb $4d$ orbitals (Ta $5d$ orbitals) and the Os $5d$ orbitals contributing the most to the density of states (DOS) at the Fermi level. There are four Fermi surface sheets (without SOC) with two of them contributing $\sim 80\%$ to the DOS at the Fermi level [17]. A combined view of all the four Fermi surface sheets of NbOsSi without SOC is shown in Fig. 3(b).

The Kramer's theorem guarantees that all the electronic bands of nonmagnetic centrosymmetric materials (Ta, Nb)OsSi are at least twofold degenerate even in the presence of SOC. We find that (Ta, Nb)OsSi have four bulk Dirac points within a ~ 10 – 20 meV energy window below the Fermi level [17]. A Dirac point in a 3D material can be considered to be composed of a superposition of two Weyl points with opposite Chern numbers [1]. The fourfold degeneracy at the Dirac point is, therefore, not topologically protected since its net Chern number is zero and will in general be lifted in the absence of any additional symmetries [1]. In the cases of (Ta, Nb)OsSi, two of the four Dirac points that lie on the $RS\bar{R}$ line ($\bar{R} \equiv -R$) are protected by the nonsymmorphic symmetry G_2 which leads to the additional twofold degeneracy. A zoomed-in view of the band structure of NbOsSi along the RS direction is shown in Fig. 3(d) and the dispersion close to the Dirac point along this line is shown in Fig. 3(e). The other two Dirac points are, however, not protected by symmetry and the surface Fermi arcs are unfortunately not clearly distinguishable [17]. Thus (Ta, Nb)OsSi are nonsymmorphic symmetry-protected Dirac semimetals expected to have characteristic spectroscopic and transport properties [2].

As a result of the exceptionally low symmetry crystal structure of (Ta, Nb)OsSi, in the strong SOC limit, there are no symmetry-allowed TRS-breaking superconducting order parameters. In the weak SOC limit, while the relevant point group $D_{2h} \otimes SO(3)$ [$SO(3)$ is the group of spin rotations in three dimensions] has four symmetry-allowed TRS-breaking superconducting instabilities, all of them have nodes [9]. Thus

clearly all the symmetry-allowed superconducting instabilities of (Ta, Nb)OsSi in the effective single band picture [24] are inconsistent with the experimental observations.

Motivated by the multiband nature of (Ta, Nb)OsSi, we phenomenologically consider an internally antisymmetric nonunitary triplet (INT) superconducting state [11] proposed in the case of LaNiGa₂, which has the same point group as (Ta, Nb)OsSi. Pairing in the INT state occurs between electrons on the same site but in two different orbitals in the nonunitary triplet channel and fermionic antisymmetry comes from orbital space. The pairing potential is $\hat{\Delta} = \hat{\Delta}_S \otimes \hat{\Delta}_B$ where the pairing potential in spin space is $\hat{\Delta}_S = (\mathbf{d} \cdot \boldsymbol{\sigma})i\tau_y$ and in orbital space is $\hat{\Delta}_B = i\tau_y$, with $\boldsymbol{\sigma}$ ($\boldsymbol{\tau}$) being the vector of Pauli matrices in spin space (orbital space). The triplet pairing is characterized by the \mathbf{d} vector: $\mathbf{d} = \Delta_a \boldsymbol{\eta}$ with $|\boldsymbol{\eta}|^2 = 1$ which is nonunitary and is characterized by the real vector $\mathbf{q} = i(\boldsymbol{\eta} \times \boldsymbol{\eta}^*) \neq 0$, and Δ_a is the pairing amplitude considered to be uniform to realize an isotropic gap observed in (Ta, Nb)OsSi. We stress that further studies are necessary to uncover the mechanism of such a pairing and Hund's rule coupling [25] is expected to play a key role due to the multiorbital nature of these materials.

There are several extended regions inside the Brillouin zone of (Ta, Nb)OsSi where two of the Fermi surface sheets are parallel and close to each other as shown in Fig. 3(b) for example. This feature is essential to stabilize the INT state and we model it by considering a simple toy model with two bands $\epsilon_{\pm}(\mathbf{k}) = \epsilon(\mathbf{k}) \pm s$ emerging from two nearly degenerate effective orbitals rigidly shifted from each other by an energy $2s$. We consider a generic dispersion $\epsilon(\mathbf{k}) = -2t[\cos(k_x) + \cos(k_y) + \cos(k_z)]$ with t being a hopping energy scale and focus on the limit $s/t \ll 1$ implying small but finite splitting between the corresponding two Fermi surfaces. To take into account the effect of SOC present in these materials, we phenomenologically consider a Rashba-type SOC. Note that although (Ta, Nb)OsSi are globally centrosymmetric, inversion symmetry is broken locally at the (Ta, Nb) sites due to the TiNiSi-type structure [26,27] which can result in a Rashba-type SOC [28,29]. Then the normal state Hamiltonian for the

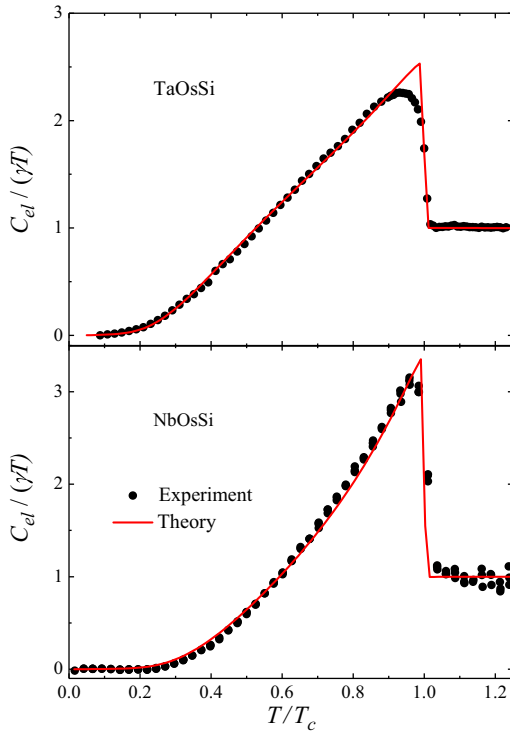


FIG. 4. Electronic specific heat. Temperature dependence of the experimentally measured electronic specific heat fitted with the theoretically computed specific heat in the INT state for the toy model with parameters $s/t = 0.1$, $\mu/t = -3.0$, and $\eta = \frac{1}{\sqrt{3}}(1, e^{i\pi/100}, e^{i101\pi/100})$. The fitting parameters for TaOsSi case are $\Delta_0/(k_B T_c) = 2.20$ and $\alpha/t = 0.15$; and for NbOsSi case are $\Delta_0/(k_B T_c) = 2.63$ and $\alpha/t = 0.20$.

toy model is $\hat{\mathcal{H}}_0 = \sum_{\mathbf{k}} \hat{c}_{\mathbf{k}}^{\dagger} \cdot H_0(\mathbf{k}) \cdot \hat{c}_{\mathbf{k}}$, defining $\hat{c}_{\mathbf{k}} = \begin{bmatrix} \tilde{c}_{\uparrow, \mathbf{k}} \\ \tilde{c}_{\downarrow, \mathbf{k}} \end{bmatrix}$ with $\tilde{c}_{p, \mathbf{k}} = \begin{bmatrix} c_{+, p, \mathbf{k}} \\ c_{-, p, \mathbf{k}} \end{bmatrix}$. $c_{\pm, p, \mathbf{k}}$ is an electron annihilation operator in the \pm band with spin $p = \uparrow$ and \downarrow , and

$$H_0(\mathbf{k}) = \sigma_0 \otimes \begin{bmatrix} \xi_+(\mathbf{k}) & 0 \\ 0 & \xi_-(\mathbf{k}) \end{bmatrix} + (k_y \sigma_x - k_x \sigma_y) \otimes \alpha \tau_x, \quad (6)$$

where $\xi_{\pm}(\mathbf{k}) = \epsilon_{\pm}(\mathbf{k}) - \mu$ with μ being the chemical potential and σ_0 is the identity matrix in spin space. The second term in Eq. (6) is a Rashba-type interorbital SOC of strength α . Although, in general, both intra- and interorbital SOC terms should be present, we can fit the specific heat data well only in the limit of interorbital SOC strength much larger than the intraorbital SOC strength, emphasizing the interorbital nature of the pairing in the INT state [17].

Using the Bogoliubov–de Gennes formalism [3], we computed the quasiparticle excitation spectrum for the toy model in the INT state considering the temperature dependence of $\Delta_a(T)$ in the form of Eq. (5). The specific heat is then computed using the temperature dependent quasiparticle spectrum to fit the experimentally measured electronic specific heat after subtracting the phonon contribution [17]. In the fitting shown in Fig. 4, we fixed $s/t \ll 1$ and T_c with the corresponding experimental values for (Ta, Nb)OsSi. Then there

are only three fitting parameters: α/t , η , and $\Delta_0/(k_B T_c)$ with $\Delta_0 \equiv \Delta_a(0)$. Figure 4 shows that the electronic specific heat for both TaOsSi [30] and NbOsSi can be fitted very well with small SOC strengths ($\alpha/t \ll 1$) in the weak coupling limit. The corresponding INT ground state has $|\mathbf{q}| = 0.03$ implying small but finite spin polarization which leads to the spontaneous magnetization in the superconducting state seen in the ZF- μ SR experiments.

III. CONCLUSIONS

We have demonstrated through detailed μ SR measurements that (Ta, Nb)OsSi belong to the rare class of TRS-breaking superconductors represented by LaNiC₂, LaNiGa₂, and UTe₂, all of which have very low-symmetry crystal structures providing a unique opportunity to constrain the superconducting order parameter from symmetries. While LaNiC₂ [8] and LaNiGa₂ [10,11] show two full gaps in the superconducting state arising from two spin channels, UTe₂ [14,31] shows point nodes and two different transitions in the superconducting state and only below the lowest transition temperature does the TRS breaking occur. In contrast, (Ta, Nb)OsSi show TRS breaking at T_c but have a full gap and low temperature thermodynamic properties similar to a conventional BCS-type superconductor as evidenced from the TF- μ SR and the specific heat data. Similarly, it will be interesting to investigate the other known isostructural superconductors in this family for possible TRS-breaking superconducting ground states, e.g., ZrOsSi which has contrasting properties than (Ta, Nb)OsSi and comparatively low T_c [32], ZrIrSi and HfIrSi [15]. We also note that (Ta, Nb)OsSi have the same structure as the ferromagnetic superconductors U(Rh, Co)Ge [27] which are proposed to realize a triplet superconducting state with equal spin pairing as in the INT state considered here. The TRS-breaking signals found in (Ta, Nb)OsSi by ZF- μ SR experiments are most likely not due to any muon induced effects, similar to other recently discovered TRS-breaking superconductors [33].

By symmetry analysis and model calculations, the phenomenology of the superconducting properties of (Ta, Nb)OsSi are found to be overall consistent with a nonunitary triplet superconducting ground state. The presence of the Dirac points close to the Fermi level promotes interband pairing and further justifies the applicability of a minimal two-band toy model to describe the low energy normal state properties [12]. The nonsymmorphic symmetries present in (Ta, Nb)OsSi can allow for nodes in the order parameter at the Brillouin zone boundaries resulting in nodal superconducting states which are clearly incompatible with the full gap observed in the experiments. However, the nonsymmorphic symmetries can lead to degeneracies in the Bogoliubov quasiparticle bands which can result in topological superconductivity [12]. Further experimental studies in these materials, such as high-resolution ARPES, are highly desirable to confirm the presence of the symmetry-protected Dirac points close to the Fermi level, when the single crystals of these materials become available. The effect of disorder and presence of any non- s -wave superconducting behaviors in (Ta, Nb)OsSi also needs to be carefully investigated. (Ta, Nb)OsSi are therefore special symmetry-protected 3D Dirac semimetal

superconductors that provide promising material platforms to investigate the rich physics arising from an interplay between topological Dirac fermions and unconventional TRS-breaking superconductivity.

All the data needed to evaluate the reported conclusions are presented in the paper and/or in the Supplemental Material. Additional data related to this paper can be available from the corresponding author upon reasonable request. The μ SR source data is available in [36].

ACKNOWLEDGMENTS

P.K.B. gratefully acknowledges the ISIS Pulsed Neutron and Muon Source of the UK Science & Technology Facilities

Council (STFC) for access to the muon beam times. S.K.G. acknowledges the Leverhulme Trust for support through the Leverhulme early career fellowship and thanks A. Agarwala, J. Quintanilla, and T. Shiroka for discussions and comments on the manuscript. X.X. acknowledges the financial support from NSFC under Grant No. 11974061 and useful discussions with X. Wan and D. Qian.

S.K.G., P.K.B., and X.X. conceived and initiated the project. C.X. and X.X. grew and characterized the samples used in this study. P.K.B. and A.D.H. conducted the muon spin rotation and relaxation experiments. B.L. and J.Z.Z. performed the first-principles calculations. S.K.G. constructed the theoretical understanding and wrote the paper with input from all the co-authors.

-
- [1] N. P. Armitage, E. J. Mele, and A. Vishwanath, Weyl and Dirac semimetals in three-dimensional solids, *Rev. Mod. Phys.* **90**, 015001 (2018).
- [2] B. Q. Lv, T. Qian, and H. Ding, Experimental perspective on three-dimensional topological semimetals, *Rev. Mod. Phys.* **93**, 025002 (2021).
- [3] S. K. Ghosh, M. Smidman, T. Shang, J. F. Annett, A. D. Hillier, J. Quintanilla, and H. Yuan, Recent progress on superconductors with time-reversal symmetry breaking, *J. Phys.: Condens. Matter* **33**, 033001 (2020).
- [4] M. Sato and Y. Ando, Topological superconductors: A review, *Rep. Prog. Phys.* **80**, 076501 (2017).
- [5] J. F. Annett, Symmetry of the order parameter for high-temperature superconductivity, *Adv. Phys.* **39**, 83 (1990).
- [6] M. Sigrist and K. Ueda, Phenomenological theory of unconventional superconductivity, *Rev. Mod. Phys.* **63**, 239 (1991).
- [7] A. D. Hillier, J. Quintanilla, and R. Cywinski, Evidence for Time-Reversal Symmetry Breaking in the Noncentrosymmetric Superconductor LaNiC_2 , *Phys. Rev. Lett.* **102**, 117007 (2009).
- [8] J. Chen, L. Jiao, J. Zhang, Y. Chen, L. Yang, M. Nicklas, F. Steglich, and H. Yuan, Evidence for two-gap superconductivity in the non-centrosymmetric compound LaNiC_2 , *New J. Phys.* **15**, 053005 (2013).
- [9] A. D. Hillier, J. Quintanilla, B. Mazidian, J. F. Annett, and R. Cywinski, Nonunitary Triplet Pairing in the Centrosymmetric Superconductor LaNiGa_2 , *Phys. Rev. Lett.* **109**, 097001 (2012).
- [10] Z. F. Weng, J. L. Zhang, M. Smidman, T. Shang, J. Quintanilla, J. F. Annett, M. Nicklas, G. M. Pang, L. Jiao, W. B. Jiang, Y. Chen, F. Steglich, and H. Q. Yuan, Two-Gap Superconductivity in LaNiGa_2 with Nonunitary Triplet Pairing and Even Parity Gap Symmetry, *Phys. Rev. Lett.* **117**, 027001 (2016).
- [11] S. K. Ghosh, G. Csire, P. Whittlesea, J. F. Annett, M. Gradhand, B. Újfalussy, and J. Quintanilla, Quantitative theory of triplet pairing in the unconventional superconductor LaNiGa_2 , *Phys. Rev. B* **101**, 100506(R) (2020).
- [12] J. R. Badger, Y. Quan, M. C. Staab, S. Sumita, A. Rossi, K. P. Devlin, K. Neubauer, D. S. Shulman, J. C. Fetting, P. Klavins *et al.*, Dirac lines and loop at the fermi level in the time-reversal symmetry breaking superconductor LaNiGa_2 , *Commun. Phys.* **5**, 22 (2022).
- [13] S. Ran, C. Eckberg, Q.-P. Ding, Y. Furukawa, T. Metz, S. R. Saha, I.-L. Liu, M. Zic, H. Kim, J. Paglione *et al.*, Nearly ferromagnetic spin-triplet superconductivity, *Science* **365**, 684 (2019).
- [14] T. Metz, S. Bae, S. Ran, I.-L. Liu, Y. S. Eo, W. T. Fuhrman, D. F. Agterberg, S. M. Anlage, N. P. Butch, and J. Paglione, Point-node gap structure of the spin-triplet superconductor UTe_2 , *Phys. Rev. B* **100**, 220504(R) (2019).
- [15] C. Benndorf, L. Heletta, G. Heymann, H. Huppertz, H. Eckert, and R. Pöttgen, NbOsSi and TaOsSi —two new superconducting ternary osmium silicides, *Solid State Sci.* **68**, 32 (2017).
- [16] E. Haque and M. A. Hossain, Elastic, electronic, thermodynamic and transport properties of XOsSi ($X = \text{Nb, Ta}$) superconductors: First-principles calculations, *J. Alloys Compd.* **739**, 737 (2018).
- [17] See Supplemental Material at <http://link.aps.org/supplemental/10.1103/PhysRevResearch.4.L012031> for details of the measurements of the crystal structure, heat capacity, and critical field, as well as for the data analysis, DFT calculation, symmetry analysis, and toy-model calculations.
- [18] R. Kubo, A stochastic theory of spin relaxation, *Hyperfine Interact.* **8**, 731 (1981).
- [19] J. E. Sonier, J. H. Brewer, and R. F. Kiefl, μ SR studies of the vortex state in type-II superconductors, *Rev. Mod. Phys.* **72**, 769 (2000).
- [20] E. H. Brandt, Properties of the ideal Ginzburg-Landau vortex lattice, *Phys. Rev. B* **68**, 054506 (2003).
- [21] R. Prozorov and R. W. Giannetta, Magnetic penetration depth in unconventional superconductors, *Supercond. Sci. Technol.* **19**, R41 (2006).
- [22] A. Carrington and F. Manzano, Magnetic penetration depth of MgB_2 , *Physica C* **385**, 205 (2003).
- [23] C. Q. Xu, B. Li, J. J. Feng, W. H. Jiao, Y. K. Li, S. W. Liu, Y. X. Zhou, R. Sankar, N. D. Zhigadlo, H. B. Wang, Z. D. Han, B. Qian, W. Ye, W. Zhou, T. Shiroka, P. K. Biswas, X. Xu, and Z. X. Shi, Two-gap superconductivity and topological surface states in TaOsSi , *Phys. Rev. B* **100**, 134503 (2019).
- [24] The nonsymmorphic symmetries present in $(\text{Ta, Nb})\text{OsSi}$, in general, can give rise to superconducting order parameters with additional symmetry required nodes along the high symmetry directions in the Brillouin zone boundaries but cannot give rise to a multicomponent order parameter to facilitate TRS breaking [12,34,35].

- [25] J. E. Han, Spin-triplet s -wave local pairing induced by Hund's rule coupling, *Phys. Rev. B* **70**, 054513 (2004).
- [26] K. Araki, T. Kohei, H. Tanaka, S. Nakamura, T. Nojima, A. Ochiai, and K. Katoh, Magnetic and transport properties of YbNiGe with a TiNiSi-type structure, *J. Phys. Soc. Jpn.* **88**, 114709 (2019).
- [27] D. Aoki, K. Ishida, and J. Flouquet, Review of u -based ferromagnetic superconductors: Comparison between UGe₂, URhGe, and UCoGe, *J. Phys. Soc. Jpn.* **88**, 022001 (2019).
- [28] S.-L. Wu, K. Sumida, K. Miyamoto, K. Taguchi, T. Yoshikawa, A. Kimura, Y. Ueda, M. Arita, M. Nagao, S. Watauchi *et al.*, Direct evidence of hidden local spin polarization in a centrosymmetric superconductor LaO_{0.55}F_{0.45}BiS₂, *Nat. Commun.* **8**, 1919 (2017).
- [29] X. Zhang, Q. Liu, J.-W. Luo, A. J. Freeman, and A. Zunger, Hidden spin polarization in inversion-symmetric bulk crystals, *Nat. Phys.* **10**, 387 (2014).
- [30] Although the experimental specific heat data for TaOsSi was shown to be fitted well by a two-gap model having more fitting parameters [23], we note from Fig. 4 that the two-band toy model in the INT ground state giving rise to a single full gap provides a very good fitting as well.
- [31] I. Hayes, D. Wei, T. Metz, J. Zhang, Y. Eo, S. Ran, S. Saha, J. Collini, N. Butch, D. Agterberg *et al.*, Multicomponent superconducting order parameter in UTe₂, *Science* **373**, 797 (2021).
- [32] W. X. Zhong, B. Chevalier, J. Etourneau, and P. Hagenmuller, Relationships between occurrence of superconductivity and crystal structure in new equiatomic ternary silicides MTSi (M = Ti, Zr, Hf and T = Ru, Os, Rh), *Solid State Commun.* **59**, 839 (1986).
- [33] B. M. Huddart, I. J. Onuorah, M. M. Isah, P. Bonfà, S. J. Blundell, S. J. Clark, R. De Renzi, and T. Lancaster, Intrinsic Nature of Spontaneous Magnetic Fields in Superconductors with Time-Reversal Symmetry Breaking, *Phys. Rev. Lett.* **127**, 237002 (2021).
- [34] S. Sumita and Y. Yanase, Unconventional superconducting gap structure protected by space group symmetry, *Phys. Rev. B* **97**, 134512 (2018).
- [35] S. Sumita, T. Nomoto, K. Shiozaki, and Y. Yanase, Classification of topological crystalline superconducting nodes on high-symmetry lines: Point nodes, line nodes, and Bogoliubov Fermi surfaces, *Phys. Rev. B* **99**, 134513 (2019).
- [36] P. K. Biswas *et al.*, (2020): STFC ISIS Neutron and Muon Source, <https://doi.org/10.5286/ISIS.E.RB1920724>.